JACS
JOURNAL OF THE AMERICAN CHEMICAL SOCIETY

Communication

pubs.acs.org/JACS

InAs Colloidal Quantum Dots Synthesis via Aminopnictogen Precursor Chemistry

Valeriia Grigel,[†,‡] Dorian Dupont,[†,‡] Kim De Nolf,[†,‡] Zeger Hens,*[,†,‡] and Mickael D. Tessier*[,†,‡]

[†]Physics and Chemistry of Nanostructures, Ghent University, 9000 Ghent, Belgium

[‡]Center for Nano and Biophotonics, Ghent University, 9000 Ghent, Belgium

Supporting Information

ABSTRACT: Despite their various potential applications, InAs colloidal quantum dots have attracted considerably less attention than more classical II-VI materials because of their complex syntheses that require hazardous precursors. Recently, aminophosphine has been introduced as a cheap, easy-to-use and efficient phosphorus precursor to synthesize InP quantum dots. Here, we use aminopnictogen precursors to implement a similar approach for synthesizing InAs quantum dots. We develop a two-step method based on the combination of aminoarsine as the arsenic precursor and aminophosphine as the reducing agent. This results in state-of-the-art InAs quantum dots with respect to the size dispersion and band gap range. Moreover, we present shell coating procedures that lead to InAs/ZnS(e) core/shell quantum dots that emit in the infrared region. This innovative synthesis approach can greatly facilitate the research on InAs quantum dots and may lead to synthesis protocols for a wide range of III-V quantum dots.

The III-V semiconductors are widely used as light-emitting or absorbing materials in optoelectronic applications. LEDs, lasers, IR photodetectors, single photon emitters and multijunction solar cells all rely on binary or multinary compounds either as bulk materials, 2D quantum wells or 0D quantum dots.[1−6] Colloidal semiconductor nanocrystals or quantum dots (QDs) are used in these applications, where their size-tunable optoelectronic properties and their suitability for printing or solution-based processing are distinctive features and major assets.[7] However, they are mostly synthesized from Pb-containing IV-VI and Cd-containing II-VI compounds for IR and visible light applications, respectively because of the reliable, efficient and relatively straightforward synthetic methods available for these materials.

Colloidal synthesis of III-V QDs is mainly restricted to InP and InAs. Whereas, the first is widely considered as the most promising alternative to Cd-based QDs for light-emitting devices,[8−11] InAs QDs cover the short-wave IR with possible applications in infrared photodetectors, photovoltaics or *in vivo* imaging.[12−14] Tris(trimethylsilyl)phosphine [$P(TMS)_3$] and tris(trimethylsilyl)arsine [$As(TMS)_3$], are the most widely used pnictide precursors for the synthesis of InP[15−20] and InAs QDs,[14,16,21−24] respectively. Both are pyrophoric and hazardous compounds that produce phosphine or arsine gas when in contact with air. In the case of InP, aminophosphines have recently emerged as a viable alternative to [$P(TMS)_3$], which results in the synthesis of QDs with similar quality while avoiding the cost and safety issues that come with the use of [$P(TMS)_3$].[25−27] In the case of InAs, innovative and safer alternatives to [$As(TMS)_3$] have been explored as well, yet these have fallen short of achieving monodisperse QD dispersions that exhibit narrow excitonic features.[28−31]

Here, we present a colloidal hot injection method to form monodisperse InAs QDs starting from tris(dimethylamino)-arsine [$As(NMe_2)_3$], which is a commercially available, cheap and safe-to-handle arsenic compound. We implement an approach inspired by the dual role played by tris-(diethylamino)phosphine [$P(NEt_2)_3$] in the synthesis of InP QDs, where it provides the phosphorus to be incorporated in the InP QDs and acts as a reducing agent.[32,33] Although a similar disproportionation does not occur for $As(NMe_2)_3$, we find that aminoarsine can be reduced to form InAs by the addition of $P(NEt_2)_3$. This approach results in state-of-the-art InAs QDs that barely contain phosphorus and have a size dispersion comparable to that obtained using $As(TMS)_3$. Finally, we present facile ZnS and ZnSe shell coating procedures, which result in the formation of InAs/ZnS and InAs/ZnSe QDs that emit in the infrared with a reasonably narrow emission line width.

To synthesize InAs QDs using $As(NMe_2)_3$, we developed a synthetic procedure where the initial steps closely resemble the method used to form InP QDs with aminophosphines.[25−27,32,33] First, indium(III) chloride and zinc(II) chloride are added to oleylamine (see Supporting Information S1 for more details). This mixture is stirred and degassed at 120 °C for 1 h under vacuum and then heated to 190 °C under inert atmosphere. Next, 1 equiv of $As(NMe_2)_3$, calculated with respect to In, is swiftly injected. Unlike the InP synthesis where the formation of InP QDs starts immediately after the addition of $P(NEt_2)_3$, the injection of $As(NMe_2)_3$ does not lead to the formation of any crystalline material. The mixture is left stirring for another 30 min, during which it turns orange. Then, 3 equiv of $P(NEt_2)_3$, with respect to In, are quickly injected in the mixture. As a result, the reaction mixture turns black within seconds, which indicates that the addition of $P(NEt_2)_3$ triggers the formation of InAs nanocrystals.

Figure 1A represents absorption spectra of the purified reaction aliquots obtained between 3 and 30 min after the injection of $P(NEt_2)_3$. All spectra exhibit a clear excitonic feature in the near IR that shifts to longer wavelengths with

Received: July 21, 2016
Published: October 5, 2016

DOI: 10.1021/jacs.6b07533
J. Am. Chem. Soc. 2016, 138, 13485−13488

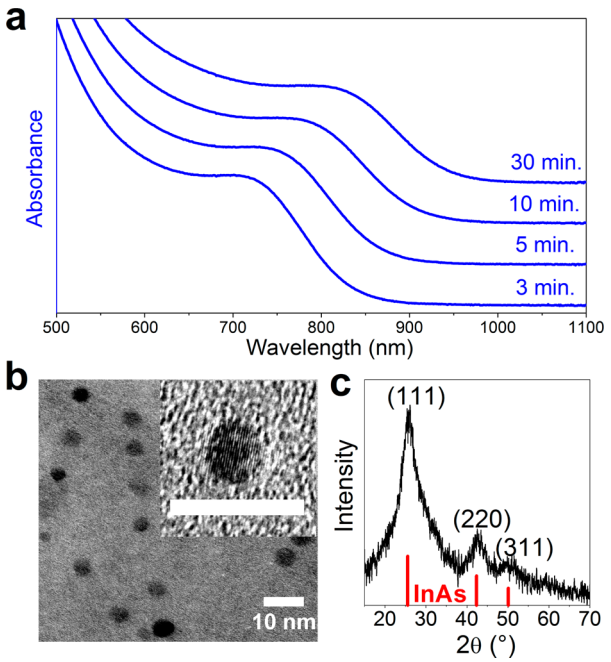

Figure 1. (a) Evolution of the absorption spectrum of InAs QDs over time for the reaction that starts after $P(NEt_2)_3$ injection. The spectra have been shifted for clarity. (b) TEM image of the resulting InAs QDs. Inset: HRTEM image of InAs QD. Both scale bars are 10 nm. (c) XRD diffractogram of the final InAs QDs.

longer reaction times; this indicates the growth of InAs QDs as time elapses. The width of the first exciton transition, which represents the size dispersion, is similar to that obtained in InAs QD syntheses with $As(TMS)_3$. It should be noted that a byproduct is formed during the reaction that makes the reaction mixture slightly turbid. All absorption spectra shown in Figure 1A were obtained for purified aliquots, where the byproduct was separated as a pellet from the InAs QDs by centrifugation (see Supporting Information S2). X-ray fluorescence spectroscopy (XRF) indicates that this byproduct mostly contains arsenic, whereas the InAs QDs recovered in the supernatant consistently feature an approximate 1:1 In:As ratio (see Supporting Information S2). The presence of this arsenic byproduct agrees with the chemical yield of the reaction, where we estimated that, depending on the synthesis, 20−50% of the $As(NMe_2)_3$ is effectively converted into InAs (see Supporting Information S3).

According to transmission electron microscopy (TEM) imaging, the purified product (see Supporting Information S4) obtained after 30 min of the reaction is composed of quasi-spherical nanocrystals (see Figure 1B) with an average diameter of ∼3.4 nm (see Supporting Information S5). A high-resolution TEM image of a single nanocrystal (Figure 1B, inset) features lattice fringes, which indicates good crystallinity. X-ray diffraction (XRD) confirms this conclusion, where diffraction peaks are observed at angles close to what is expected for zinc-blende InAs QDs, as shown in Figure 1C. A detailed comparison, however, shows a small but systematic shift of all peaks to higher angles relative to bulk InAs values. The (111) peak, for example, is centered at 25.9° instead of 25.5°. Although such shifts could be attributed to the formation of an In(As,P) alloy, this is not confirmed by elemental analysis. Energy Dispersive X-ray spectroscopy on the same sample indicates that the nanocrystals contain negligible amounts of phosphorus (see Supporting Information S6).

To understand the mixed aminopnictogen approach, it is useful to revert to the current understanding of the amino-phosphine-based synthesis of InP QDs.[32,33] The conversion of $P(NEt_2)_3$ into InP involves two major steps. Upon its injection in a reaction mixture composed of indium and zinc halides, which is dissolved in a primary amine, $P(NEt_2)_3$ undergoes a series of transamination reactions. In other terms, the diethylamino groups are replaced by oleylamino groups concomitant with the release of diethylamine from the reaction mixture:

$$P(NEt_2)_3 + 3OlNH_2 \rightarrow P(NHOl)_3 + 3Et_2NH \quad (1)$$

Here, Ol represents an oleyl moiety. The actual formation of InP occurs through a disproportionation of this transaminated aminophosphine:[32,33]

$$InCl_3 + 4P(NHOl)_3 \rightarrow InP + 3P(NHOl)_4Cl \quad (2)$$

In this equation, one phosphorus equivalent undergoes a reduction to P(−III), whereas three phosphorus equivalents are oxidized to P(+V).

As described before, the InAs QDs synthesis presented here follows a two-step approach, where the first step involves the injection of $As(NMe_2)_3$ in the reaction mixture containing indium and zinc halides dissolved in oleylamine. Scrubbing the reaction exhaust after $As(NMe_2)_3$ injection with an aqueous solution of $CuSO_4$ results in the formation of $Cu(OH)_2$. This indicates that the exhaust contains a basic gas that is formed during the reaction (see Supporting Information S7), which is similar to what happens after the injection of $P(NEt_2)_3$ during the synthesis of InP QDs. This gas is presumably dimethylamine according to the $As(NMe_2)_3$ equivalent of the transamination reaction (eq 1):

$$As(NMe_2)_3 + 3OlNH_2 \rightarrow As(NHOl)_3 + 3Me_2NH \quad (3)$$

In contrast to the aminophosphine-based synthesis of InP QDs (eq 2), no InAs is formed during this first step of the procedure. This possibly occurs because $As(NHOl)_3$ is not a strong enough reducing agent.

The second step is the addition of $P(NEt_2)_3$. As the reaction mixture contains an excess of oleylamine, transamination can be expected again for this aminophosphine species (eq 1). Because the formation of InAs QDs begins at this point, the transaminated aminophosphine presumably acts as the reducing agent, which is similar to its role in the synthesis of InP QDs. The formation reaction of InAs QDs can then be summarized as follows:

$$InCl_3 + As(NHOl)_3 + 3P(NHOl)_3 \rightarrow InAs + 3P(NHOl)_4Cl \quad (4)$$

Figure 2 represents ^{31}P NMR spectra of reaction aliquots taken during the synthesis of InAs QDs; the aliquots were obtained 10 s and 30 min after $P(NEt_2)_3$ injection. The spectrum of $P(NEt_2)_3$ is included as a reference. Clearly, $P(NEt_2)_3$ has almost completely disappeared after just 10 s of reaction, again confirming its rapid transamination upon injection in the oleylamine-based reaction mixture (eq 1). The several resonances at approximately 110 ppm represent transaminated aminophosphines.[32] Finally, the resonance at 29 ppm has previously been attributed to an oleylamino phosphonium salt that is also formed as a byproduct in the

DOI: 10.1021/jacs.6b07533
J. Am. Chem. Soc. 2016, 138, 13485−13488

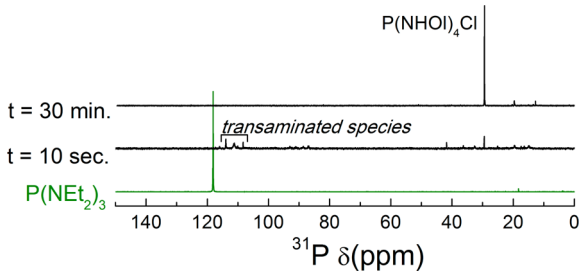

Figure 2. ^{31}P NMR spectra of $P(NEt_2)_3$ and two aliquots obtained at the indicated time after aminophosphine precursor injection during the synthesis of InAs QDs.

aminophosphine-based formation of InP QDs.[32,33] The dominant presence of this phosphonium salt at the end of the reaction confirms that $P(NEt_2)_3$ is an effective reducing agent that enables the formation of InAs QDs from $InCl_3$ and $As(NMe_2)_3$, according to eq 4. We thus conclude that the reduction of the initial As(+III) compound to As(−III) is enabled by the oxidation of three phosphorus equivalents from P(+III) to P(+V). It should be underlined that we do not observe evidence of the formation of InP or In(As,P) alloyed QDs when using 3 equiv of $P(NEt_2)_3$. This indicates that $InCl_3$ binds preferentially to aminoarsine. This hypothesis is confirmed by using different amounts of $P(NEt_2)_3$ (see Supporting Information S8). Upon injection of only 1 or 2 equiv of $P(NEt_2)_3$, amounts leading to InP QDs in the absence of $As(Me_2)_3$, neither InAs nor InP is formed. Hence, no $InCl_3$ is available for the formation of InP while the amount of $P(NEt_2)_3$ is insufficient to form As(−III). When 6 equiv of $P(NEt_2)_3$ is added, mixed In(As,P) QDs are formed, yet their 5:1 As:P atomic ratio again confirms the preferential reduction of aminoarsine in this reaction.

We found that InAs core QDs synthesized using aminopnictogen precursor chemistry barely show any photoluminescence. A shell coating therefore seems imperative for light-emitting applications. We found that ZnS and ZnSe shells can be grown by a one-pot method where $Zn(Stearate)_2$, dispersed in octadecene, and stoichiometric *tri*-octylphosphine sulfide (TOP-S) or selenide (TOP-Se) are added as ZnS or ZnSe precursors to the reaction mixture (see Supporting Information S9). In the Supporting Information S10, we present TEM pictures of InAs/ZnS and InAs/ZnSe QDs obtained at the end of the shell coating reaction. The TEM analysis of the obtained QDs is difficult as the QDs tend to aggregate. Although the InAs/ZnS QDs appear spherical, a tetrahedral shape can be distinguished in some areas for the InAs/ZnSe QDs, which is similar to that of InP/ZnSe QDs.[26] According to XRD analysis, both InAs/ZnS and InAs/ZnSe QDs have a zinc-blende structure (Supporting Information S11), where the diffraction peaks have shifted toward the ZnS or ZnSe positions.

Figure 3a,b shows absorbance and photoluminescence spectra of InAs/ZnS and InAs/ZnSe core/shell QDs. Compared to the original InAs QDs, a small redshift, more pronounced for ZnSe shells, of the exciton is observed after shell growth, which is typical of a type-I structure. Photoluminescence bands with a peak in the range of 900−1100 nm and a line width of 100−150 nm are commonly observed. For both systems, the photoluminescence quantum yield (PLQY) as determined using an integrating sphere,[34] amounts to 5−10%. These emission characteristics are similar to what is

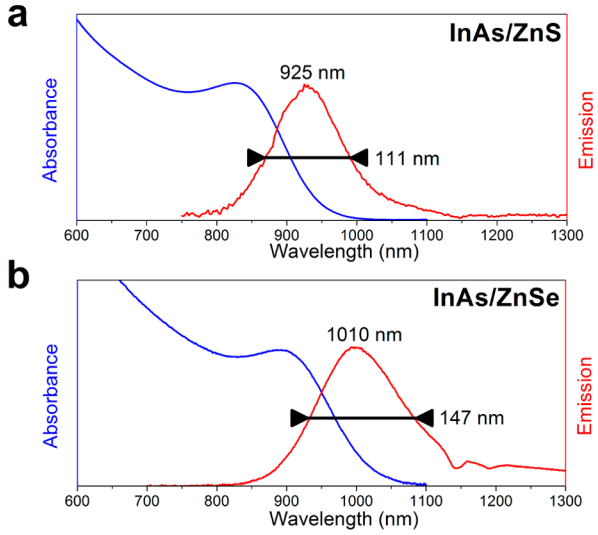

Figure 3. Absorption and emission spectra of (a) InAs/ZnS and (b) InAs/ZnSe QDs.

typically observed for InAs/ZnS(e) QDs obtained via As(TMS)$_3$ (emission line width: ∼200 nm, PLQY: 7−20%).[22] A higher PLQY has been reported for other InAs-based core/shell systems, such as InAs/CdSe,[23] InAs/InP/ZnSe[14] and InAs/(Cd,Zn)S.[13] Such differences have been attributed to the smaller lattice mismatch between the core and the shell for these structures compared to InAs/ZnS(e).[13,14,23]

In summary, we have shown that high-quality InAs colloidal QDs can be synthesized from cheap, convenient and safe-to-use aminopnictogen precursors. The reaction protocol proposed uses aminoarsine as the arsenic precursor and aminophosphine as the reducing agent. The latter is confirmed by the conversion of the P(+III) aminophosphine to a P(+V) phosphonium salt during the reaction. Easy-to-implement ZnS and ZnSe shell coating procedures have been demonstrated, which lead to the formation of InAs-based core/shell QDs that emit in the near-infrared. The approach developed here significantly broadens the perspective of synthesizing III-V QDs using aminopnictogen precursors. First, such two-step strategies may offer a further breakthrough in the synthesis of colloidal nanocrystals from other III-V compounds, such as InSb or GaAs. Second, using a more appropriate reducing agent could suppress the side reaction that was observed during the formation of InAs and lead to the formation of nanocrystals with an improved size dispersion. In this respect, a synthesis of InAs QDs that used diisobutylaluminum hydride as a reducing agent was recently published.[35] This further underscores the effectiveness of these two-step synthesis techniques, where nanocrystal formation is made possible by the introduction of a reducing agent.

■ ASSOCIATED CONTENT

Supporting Information

The Supporting Information is available free of charge on the ACS Publications website at DOI: 10.1021/jacs.6b07533.

Synthesis protocol for InAs QDs, separation and elemental analysis of the byproduct and InAs QDs, reaction chemical yield evaluation, purification method of the QDs for TEM analysis, histogram of size distribution of InAs QDs after purification, XRD and EDX analysis of InAs QDs, gas analysis of the reaction between $As(NMe_2)_3$ and oleylamine, aminoarsine:aminophos-

DOI: 10.1021/jacs.6b07533
J. Am. Chem. Soc. 2016, 138, 13485−13488

phine ratio study, InAs/ZnS and InAs/ZnSe QDs protocols, TEM pictures of InAs/ZnS and InAs/ZnSe QDs, and XRD diffractograms of InAs/ZnS and InAs/ZnSe QDs (PDF)

AUTHOR INFORMATION

Corresponding Authors

*Z.H. zeger.hens@ugent.be

*M.T. mickael.tessier@ugent.be

Notes

The authors declare no competing financial interest.

ACKNOWLEDGMENTS

The authors are grateful to J. Maes, K. Haustraete and W. Walravens for their help with material characterization. V.G., M.D.T. and D.D. acknowledge the Instituut voor de Aanmoediging van Innovatie door Wetenschap en Technologie in Vlaanderen for funding (IWT-SBO Lumicor, IWT-SBO MIRIS). Z.H. acknowledges support by the European Comission via the Marie-Sklodowska Curie action Phonsi (H2020-MSCA-ITN-642656), the Belgian Science Policy office (IAP 7.35, photonics@be), and Ghent University (GOA 01G01513) for funding.

REFERENCES

(1) Mokkapati, S.; Jagadish, C. *Mater. Today* **2009**, *12*, 22.
(2) Tanabe, K. *Energies* **2009**, *2*, 504.
(3) Yin, Z.; Tang, X. *Solid-State Electron.* **2007**, *51*, 6.
(4) Kish, F.; Nagarajan, R.; Welch, D.; Evans, P.; Rossi, J.; Pleumeekers, J.; Dentai, A.; Kato, M.; Corzine, S.; Muthiah, R.; Ziari, M.; Schneider, R.; Reffle, M.; Butrie, T.; Lambert, D.; Missey, M.; Lal, V.; Fisher, M.; Murthy, S.; Salvatore, R.; Demars, S.; James, A.; Joyner, C. *Proc. IEEE* **2013**, *101*, 2255.
(5) Gayral, B.; Gérard, J. M. *Phys. E* **2000**, *7*, 641.
(6) Santori, C.; Fattal, D.; Vuckovic, J.; Solomon, G. S.; Yamamoto, Y. *New J. Phys.* **2004**, *6*, 89.
(7) Kovalenko, M. V.; Manna, L.; Cabot, A.; Hens, Z.; Talapin, D. V.; Kagan, C. R.; Klimov, X. V. I; Rogach, A. L.; Reiss, P.; Milliron, D. J.; Guyot-sionnnest, P.; Konstantatos, G.; Parak, W. J.; Hyeon, T.; Korgel, B. A.; Murray, C. B.; Heiss, W. *ACS Nano* **2015**, *9*, 1012.
(8) Ziegler, J.; Xu, S.; Kucur, E.; Meister, F.; Batentschuk, M.; Gindele, F.; Nann, T. *Adv. Mater.* **2008**, *20*, 4068.
(9) Kim, S.; Kim, T.; Kang, M.; Kwak, S. K.; Yoo, T. W.; Park, L. S.; Yang, I.; Hwang, S.; Lee, J. E.; Kim, S. K.; Kim, S. W. *J. Am. Chem. Soc.* **2012**, *134*, 3804.
(10) Lee, S.-H.; Lee, K.-H.; Jo, J.-H.; Park, B.; Kwon, Y.; Jang, H. S.; Yang, H. *Opt. Mater. Express* **2014**, *4*, 1297.
(11) Yang, S. J.; Oh, J. H.; Kim, S.; Yang, H.; Do, Y. R. *J. Mater. Chem. C* **2015**, *3*, 3582.
(12) Lee, S. H.; Jung, C.; Jun, Y.; Kim, S.-W. *Opt. Mater. (Amsterdam, Neth.)* **2015**, *49*, 230.
(13) Allen, P. M.; Liu, W.; Chauhan, V. P.; Lee, J.; Ting, A. Y.; Fukumura, D.; Jain, R. K.; Bawendi, M. G. *J. Am. Chem. Soc.* **2010**, *132*, 470.
(14) Xie, R.; Chen, K.; Chen, X.; Peng, X. *Nano Res.* **2008**, *1*, 457.
(15) Micic, O. I.; Sprague, J. R.; Curtis, C. J.; Jones, K. M.; Machol, J. L.; Nozik, A. J.; Giessen, H.; Fluegel, B.; Mohs, G.; Peyghambarian, N. *J. Phys. Chem.* **1995**, *99*, 7754.
(16) Battaglia, D.; Peng, X. *Nano Lett.* **2002**, *2*, 1027.
(17) Li, L.; Reiss, P. *J. Am. Chem. Soc.* **2008**, *130*, 11588.
(18) Gary, D. C.; Cossairt, B. M. *Chem. Mater.* **2013**, *25*, 2463.
(19) Allen, P. M.; Walker, B. J.; Bawendi, M. G. *Angew. Chem., Int. Ed.* **2010**, *49*, 760.
(20) Tamang, S.; Lincheneau, C.; Hermans, Y.; Jeong, S.; Reiss, P. *Chem. Mater.* **2016**, *28*, 2491.
(21) Guzelian, A. A.; Banin, U.; Kadavanich, A. V.; Peng, X.; Alivisatos, A. P. *Appl. Phys. Lett.* **1996**, *69*, 1432.
(22) Cao, Y. W.; Banin, U. *J. Am. Chem. Soc.* **2000**, *122*, 9692.
(23) Xie, R.; Peng, X. *Angew. Chem., Int. Ed.* **2008**, *47*, 7677.
(24) Aharoni, A.; Mokari, T.; Popov, I.; Banin, U. *J. Am. Chem. Soc.* **2006**, *128*, 257.
(25) Song, W.-S.; Lee, H.-S.; Lee, J. C.; Jang, D. S.; Choi, Y.; Choi, M.; Yang, H. *J. Nanopart. Res.* **2013**, *15*, 1750.
(26) Tessier, M. D.; Dupont, D.; De Nolf, K.; De Roo, J.; Hens, Z. *Chem. Mater.* **2015**, *27*, 4893.
(27) Kim, K.; Yoo, D.; Choi, H.; Tamang, S.; Ko, J.-H.; Kim, S.; Kim, Y.-H.; Jeong, S. *Angew. Chem., Int. Ed.* **2016**, *55*, 3714.
(28) Das, A.; Shamirian, A.; Snee, P. T. *Chem. Mater.* **2016**, *28*, 4058.
(29) Green, M.; Norager, S.; Moriarty, P.; Motevalli, M.; O'Brien, P. *J. Mater. Chem.* **2000**, *10*, 1939.
(30) Malik, M. A.; O'Brien, P.; Helliwell, M. *J. Mater. Chem.* **2005**, *15*, 1463.
(31) Uesugi, H.; Kita, M.; Omata, T. *J. Cryst. Growth* **2015**, *416*, 134.
(32) Tessier, M. D.; De Nolf, K.; Dupont, D.; Sinnaeve, D.; De Roo, J.; Hens, Z. *J. Am. Chem. Soc.* **2016**, *138*, 5923.
(33) Buffard, A.; Dreyfuss, S.; Nadal, B.; Heuclin, H.; Xu, X.; Patriarche, G.; Mézailles, N.; Dubertret, B. *Chem. Mater.* **2016**, *28*, 5925.
(34) Aubert, T.; Soenen, S. J.; Wassmuth, D.; Cirillo, M.; Van Deun, R.; Braeckmans, K.; Hens, Z. *ACS Appl. Mater. Interfaces* **2014**, *6*, 11714.
(35) Srivastava, V.; Janke, E. M.; Diroll, B. T.; Schaller, R. D.; Talapin, D. V. *Chem. Mater.* **2016**, *28*, 6797.

DOI: 10.1021/jacs.6b07533
J. Am. Chem. Soc. 2016, 138, 13485−13488